GEOLOGICA CARPATHICA, AUGUST 2012, 63, 4, 295–305 doi: 10.2478/v10096-012-0023-5

Neogene uplift and erosion in the Alpine Foreland Basin (Upper Austria and Salzburg)

JUERGEN GUSTERHUBER[1], ISTVÁN DUNKL[2], RALPH HINSCH[3], HANS-GERT LINZER[3] and REINHARD F. SACHSENHOFER[1]

[1]Department of Applied Geosciences and Geophysics, Peter-Tunner-Strasse 5, A-8700 Leoben, Austria; juergen.gusterhuber@gmail.com; reinhard.sachsenhofer@unileoben.ac.at
[2]Sedimentology and Environmental Geology, Geoscience Center, University of Göttingen, Goldschmidtstraße 3, D-37077 Göttingen, Germany; istvan.dunkl@geo.uni-goettingen.de
[3]RAG Rohöl-Aufsuchungs Aktiengesellschaft, Schwarzenbergplatz 16, A-1015 Vienna, Austria; ralph.hinsch@rag-austria.at; hans-gert.linzer@rag-austria.at

(Manuscript received December 14, 2011; accepted in revised form March 13, 2012)

Abstract: In the present paper we apply a multi-technique approach (shale compaction data, seismic stratigraphy, isopach maps, moisture content of lignite, fission track data) to assess timing and amount of uplift and erosion of the Alpine Foreland Basin. The combination of the different techniques allows us to discriminate the effects of two different erosion events during the Neogene: (1) Seismic stratigraphy and isopach maps indicate a Karpatian (Early Miocene) regional tilting of the basin to the west (slope of about 0.5 %) and a minor erosion phase. (2) Moisture content of lignite combined with fission track data provides evidence for extensive regional uplift after deposition of Late Miocene fluvial deposits. It is estimated that sediments, 500 to 900 m thick, have been eroded. Shale compaction data derived from sonic logs indicates additional uplift of the eastern part of the basin (near the river Enns). Here, 300 to 1000 m of sediments were additionally eroded (giving a total erosion of about 1000 to 1900 m!), with a general increase of erosion thickness towards the northeast. While the regional uplift is probably related to isostatic rebound of the Alps after termination of thrusting, the local uplift in the east could be affected by Late Neogene E-W compressional events within the Alpine-Pannonian system. Both, tilting and erosion influence the hydrocarbon habitat in the Molasse Basin (tilting of oil–water contacts, PVT conditions, biodegradation).

Key words: Neogene, Alpine Foreland Basin, uplift, erosion, shale compaction, seismic stratigraphy, fission track data.

Introduction

Extensive oil and gas exploration activities in the Austrian and German sectors of the Alpine Foreland Basin contributed greatly to a detailed image of the subsurface. But while the stratigraphy, architecture and evolution of the basin fill are reasonably well understood (e.g. Nachtmann & Wagner 1987; Bachmann et al. 1987; Wagner 1996, 1998; Kuhlemann & Kempf 2002) knowledge on Neogene uplift and erosion processes within the basin is largely missing (Genser et al. 2007).

This is in contrast to the Swiss sector of the Alpine Foreland Basin, where several authors, including Schegg & Leu (1998) and Cederbom et al. (2011) investigated the amount and timing of erosion. Beside this difference in knowledge a significantly higher amount of erosion in the western part of the Alpine Foreland Basin is proven.

The investigation of erosional events in the eastern part of the Alpine Foreland has been initiated in the course of a basin and petroleum systems modelling study in Upper Austria and Salzburg (Gusterhuber et al. 2011) which showed that erosion and uplift may have strong effects on timing of generation, charging and preservation of hydrocarbons.

Different techniques, including shale compaction, lignite compaction, and low temperature thermochronology are applied in the present paper with the objective of assessing the timing and magnitude of Neogene uplift and erosion.

Geological setting

The Alpine Foreland Basin (Molasse Basin) of Salzburg and Upper Austria represents a part of the Alpine-Carpathian Foredeep (Fig. 1). It was formed due to the collision of the Alpine orogenic system with the southern margin of the European platform in the Middle Paleogene. The basin displays a typical asymmetrical peripheral foreland basin in terms of an increasing basin depth towards the Alpine thrust front in the south and a gradual shallowing and narrowing trend from west to east towards the spur of the Bohemian Massif (Malzer et al. 1993).

The crystalline basement of the Molasse Basin is overlain by an incomplete cover of Late Paleozoic and Mesozoic rocks (Fig. 2). Erosion during the latest Cretaceous left a peneplain on which the Tethyan Sea progressively transgressed during the latest Eocene and earliest Oligocene times. At this stage the Molasse Basin was formed and became the pelagic Alpine Foredeep. The area rapidly subsided to deep-water conditions accompanied by the development of an E-W trending fault network due to downward bending of the European Plate (Wagner 1996, 1998).

Approximately at the Eocene-Oligocene boundary, strong tectonic activities changed the Eurasian configuration and separated the Tethyan Sea into the Paratethys in the north and the Mediterranean in the south. The closure of the Indo-Pacific

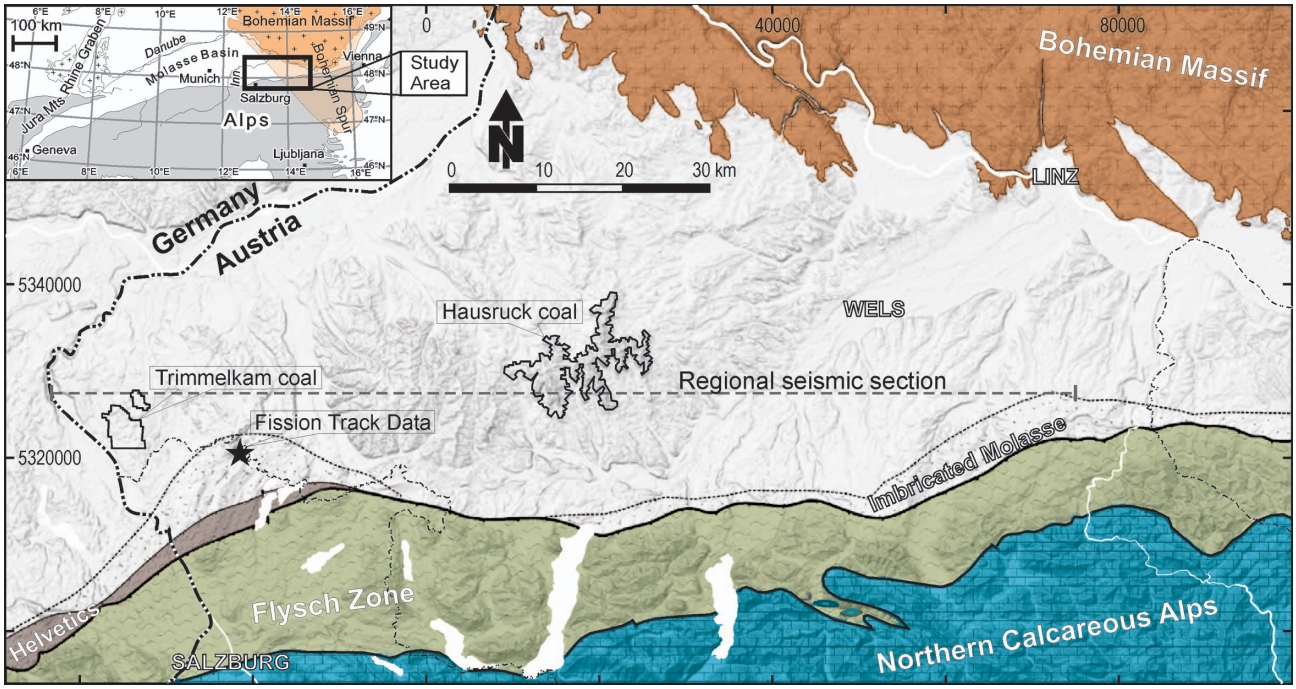

Fig. 1. Simplified geological map of the study area superposed on shaded relief digital elevation model created from SRTM data (SRTM 2004). The positions of data discussed in the paper are given: The regional seismic section (Fig. 5), the well position of the Fission Track samples (Per-001) and the outlines of coal mining areas (samples for Lignite diagenesis analysis; Fig. 6). The inset map (top left) shows the position of the study area in the frame of the Northern Alpine Foreland.

connection caused the first isolation of the Paratethys. Deep basins with reduced circulation and oxygen deficient bottom conditions led to the deposition of marine organic matter-rich rocks, which are the source for thermogenic hydrocarbons in the Molasse Basin (Schoeneck, Dynow, Eggerding Formations; Schulz et al. 2002, 2005; Sachsenhofer et al. 2010). Thereafter new seaways opened from the Mediterranean and the Indian Ocean to the Paratethys causing normal marine oxygenated bottom conditions (Rögl 1999). In the Late Oligocene and earliest Miocene, uplift of the Alps caused increased sediment discharge from the south correlating with a distinct eustatic sea-level fall and the incision of a slope-parallel (E–W) trough by strong bottom currents (Krenmayer 1999) and corresponding widespread deposition of deep-water channels (Linzer 2002; De Ruig & Hubbard 2006). Contemporaneous sediments of the deep-water Lower and Upper Puchkirchen Formation (Egerian) are represented by coal-bearing continental to brackish clays and sands along the northern margin of the study area (Krenmayer 1999). In the Early Burdigalian (Eggenburgian), deep-water conditions persisted during deposition of the Hall Formation when a gradual transition to shallow-water sedimentation occurred with continental slope-delta progradation across the area (Hinsch 2008; Hubbard et al. 2009).

Marine conditions continued during the Ottnangian with the deposition of the Innviertel Group (e.g. Faupl & Roetzel 1987; Grunert et al. 2010). While fully-marine, tidal dominated silts and sands represent Early and Middle Ottnangian transgressive and highstand phases, brackish-fluvial sediments of the Oncophora Beds were deposited during a Late Ottnangian regressive phase (Rögl 1998; Grunert et al. 2012). As a result of their brackish character, a separation of the Oncophora Beds from the Innviertel Group is under discussion (Rupp et al. 2008).

Following a major hiatus, a thick succession of coal-bearing clays, sands and fluviatile gravels was deposited (Upper Freshwater Molasse). In Upper Austria, freshwater deposition commenced in the Early Badenian in the western Trimmelkam area (Rein in Weber & Weiss 1983; see Fig. 1 for location) and became gradually younger towards the east. In the Hausruck area Badenian and Sarmatian deposits are missing and Pannonian coal measures directly overlie Ottnangian deposits (Czurda 1978). This indicates that sedimentation proceeded eastwards on a tilted surface and agrees with the observation that coal-bearing beds in the Hausruck area were deposited in erosional depressions within a generally southwestward dipping peneplain (Pohl 1968; Groiss 1989). The youngest preserved deposits in the Upper Austrian part of the Molasse Basin are the fluviatile Hausruck Gravels. These are poorly dated, but generally attributed to the Pannonian (Rupp et al. 2008). Obviously, today the Molasse Basin is an erosional domain.

Badenian lignite seams have been mined in the western Trimmelkam district, whereas Pannonian lignite was exploited in the Hausruck mining district (Weber & Weiss 1983).

Data and methods

The study is based on seismic data, well log data, moisture content of lignite and fission track data.

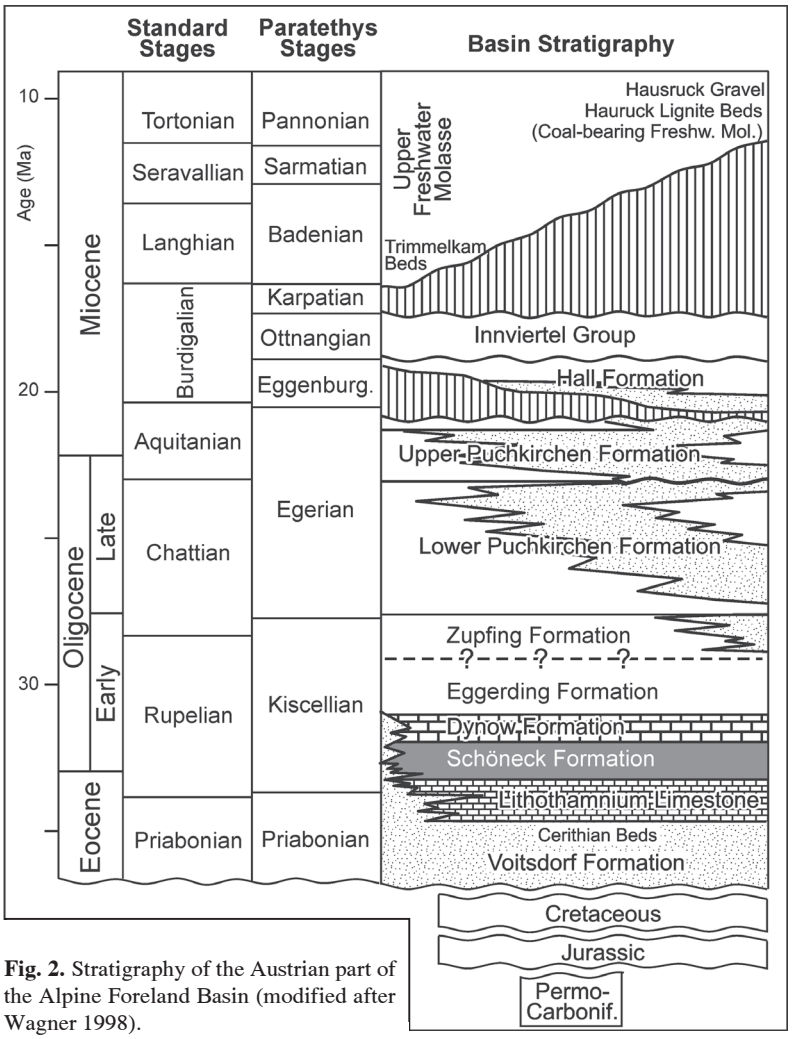

Fig. 2. Stratigraphy of the Austrian part of the Alpine Foreland Basin (modified after Wagner 1998).

Seismic data

Large parts of the Upper Austrian part of the Molasse Basin are covered by high quality 3D seismic data. These data have been used to outline progradational patterns within the Hall Formation. In addition, stratigraphic information from the wells was used to map the base of the Innviertel Group (representing a significant part of the Upper Marine Molasse) and the base of the Upper Freshwater Molasse, as well as thickness of sediments between both. These shallow stratigraphic markers are often picked from mud logging or well log response and not always confirmed by micropaleontology. Thus, some uncertainties in the order of 10th of meters might be regarded to the individual selection. To moderate uncertainties, the created surfaces have been smoothed on a 1×1 km grid. The created surface therefore reflects the trends of the stratigraphic surfaces.

Shale compaction/Log data

Shale compaction is irreversible and directly related to overburden stress (burial depth) if pore pressure is hydrostatic. Obviously, deeply buried shales which reached a given depth will be more strongly compacted after uplift and erosion than shales at the same depth in an area without erosion. Thus, in an area with hydrostatic pressure shale compaction trends can be used to estimate the thickness of eroded rocks (Magara 1976, 1980). The amount of compaction can be quantified from the sonic log because sonic transit time is a result of interaction between porosity and the rock matrix in a uniform lithology like shales.

In the present study sonic logs from 80 boreholes have been used to quantify erosion.

Moisture content of lignite

As in the case of shale, the compaction of low-rank coal is mainly controlled by burial depth and increasing overburden pressure. The moisture content of lignite (on an ash free basis, af) provides a great tool to monitor this process. A data set from (as received) lignite in the Lower Rhine Embayment (Kothen & Reichenbach 1981) confirms this relation (Fig. 6). Because the ash yield of lignite from the Lower Rhine Embayment is typically only 1 to 2 %, the difference between moisture contents on an ash received and an ash free basis is negligible. Thus, in the present paper the moisture depth trend in Fig. 6 is used to estimate the thickness of overburden rocks in the Hausruck and Trimmelkam areas. Analytical data from 31 pillar samples from the Pannonian-age Hausruck lignite have been reported by Pohl (1968). Data from the Badenian-age Trimmelkam lignite have been provided by Weber & Weiss (1983). Both data sets have been used to calculate moisture contents (af).

Low temperature thermochronology

In order to detect the magnitude and timing of the post-depositional burial temperature we have performed low temperature thermochronology using apatite fission track and apatite (U-Th)/He methods (AFT and AHe, respectively). Several samples from different stratigraphic horizons have been investigated, but only one sample from well Per-001 (see Fig. 1; 1600 m depth) yielded suitable contents of apatite.

AFT

The apatite crystals were embedded in epoxy resin and the crystal mounts were polished by diamond using a five-step procedure. In order to reveal the spontaneous tracks the apatite mounts were etched by 5.5 N nitric acid at 21 °C for 20 seconds (Donelick et al. 1999). Neutron irradiations were performed at the nuclear reactor of Oregon State University, USA. The external detector method was used (Gleadow 1981); after irradiation the induced fission tracks in the mica detectors were revealed by etching in 40% HF for 35 min.

Track counts were made with a Zeiss-Axioskop microscope — computer-controlled stage system (Dumitru 1993), with a magnification of 1000×. The FT ages were determined by the zeta method (Hurford & Green 1983) using the age standards listed in Hurford (1998).

AHe

Only single crystal aliquots were dated; and only inclusion and fissure-free specimens with a well-defined external morphology were used. The shape parameters were determined and archived by multiple digital microphotographs. The ejection correction factor (Ft) was determined for the single crystals by the method of Farley (2002). The crystals were wrapped in ca. 1×1 mm sized platinum capsules and degassed by heating an infrared diode laser. The extracted gas was purified using a SAES Ti-Zr getter at 450 °C. The chemically inert noble gases and a minor amount of other gases were expanded into a Hiden triple-filter quadrupole mass spectrometer equipped with a positive ion counting detector. No analysed crystal exhibited residual gas >1 % after the first extraction. Following degassing, samples were retrieved from the gas extraction line, spiked with calibrated 230 Th and 233 U solutions and dissolved in a 2% HNO_3+0.05% HF acid mixture in teflon vials. Each sample batch was prepared with a series of procedural blanks (including Pt tube blanks) and spiked normals to check the purity and calibration of the reagents and spikes. Spiked solutions were analysed as 0.5 or 0.8 ml of ~0.5 ppb U-Th solutions by isotope dilution on a Perkin Elmer Elan DRC II ICP-MS with a APEX microflow nebulizer. Procedural U and Th blanks by this method are usually very stable and below 1.5 pg. Sm, Pt and Ca were determined by external calibration.

Results

Shale compaction

Figure 3 shows the depth trend of the sonic transit times for the Eggerding Formation. In order to minimize effects due to lithology variations, only the shaly upper part of the Eggerding Formation, which is typically characterized by uniform transit times, is considered (see inset in Fig. 3). The data, which are from wells located in different parts of the study area (Fig. 4a), follow a well-defined exponential trend, which reflects increasing shale compaction with burial depth. Actually exponential relations are the most widely accepted equation for describing shale compaction (Issler 1992), although linear shale compaction trends have also been reported (e.g. Wells 1990).

It is important to note, that the Eggerding Formation shows relatively low transit times and significant deviations from the "normal" exponential compaction curve in some shallow wells. All "abnormal" wells are located in the eastern part of the study area. A comparison of the gamma ray logs from the "abnormal" Steyr W 1 and the "normal" Kemating 1 wells (inset in Fig. 3) suggests that this is not due to an eastward increase in sand content, but due to overcom-

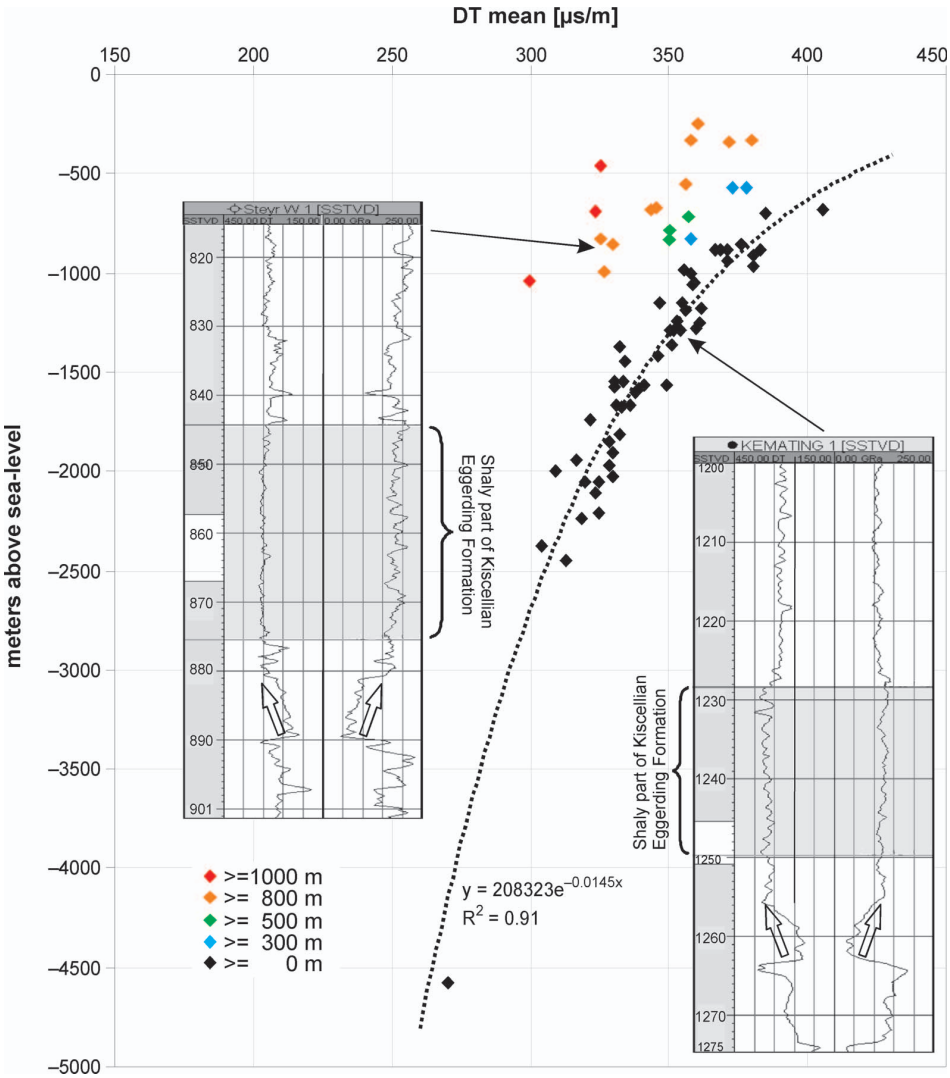

Fig. 3. Transit-time of the shaly interval of the Oligocene Eggerding Formation vs. meters above sea-level for several wells.

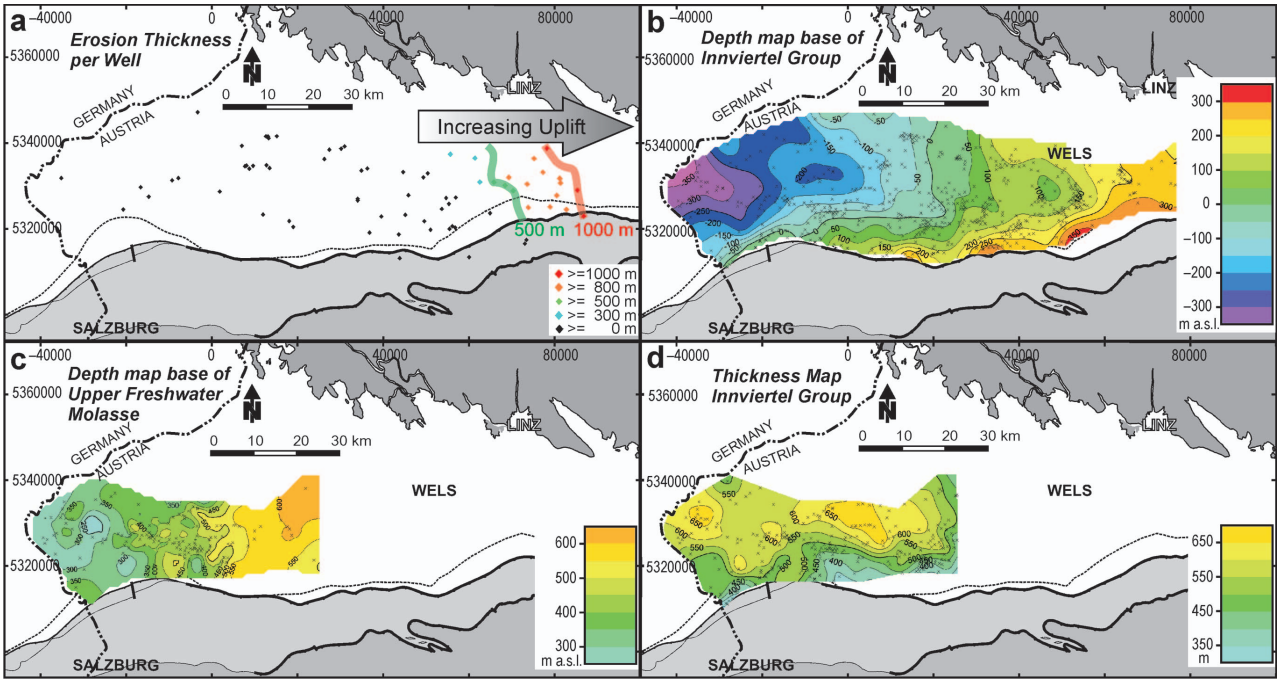

Fig. 4. Results from different analysis, displayed on a study area map (for background geology see Figure 1). **a** — Estimated amount of erosion from shale compaction analysis of the Eggerding Formation in several wells (small diamonds). Hand-contoured isolines mark 500 m (green) and 1000 m (red). **b** — Interpolated present day depth map (meters above sea-level — m a.s.l.) of the base of Innviertel Group from well data (small dots). **c** — Interpolated present day depth map of the base of Upper Freshwater Molasse from well data (small dots). **d** — Interpolated thickness of the Innviertel Group from well data (small dots). In order to determine the thickness of the Innviertel Group before deposition of the Upper Freshwater Molasse, only areas where the Innviertel Group is overlain by the latter are considered.

paction. Consequently, we conclude that the easternmost part of the study area experienced more uplift and erosion than its main part. The vertical deviation of the measured data points from the normal compaction trend allows a quantification of the additional amount of erosion. These data range from 300 to 1000 m and are mapped in Fig. 4a.

Seismic stratigraphic aspects of the Hall Formation

Eggenburgian sediments of the Hall Formation exhibit progradational patterns, which indicate eastward sediment transport (Fig. 5). It is reasonable to assume that during progradation, the top of the sedimentary package (toplap surface) was horizontal. Thus, the observed present-day inclination of the toplap surface was horizontal during its formation. Consequently, the observed pattern implies a distinct eastward tilting of the basin since the Eggenburgian. The seismic section flattened to the base of the Innviertel Group (=top Hall Formation) displays the original geometry before the tilting event (Fig. 5).

Elevation of base Innviertel Group and base Upper Freshwater Molasse

On the basis of 3D seismic data and information from 698 wells, depth-maps of base Innviertel Group (=top Hall Formation), base Upper Freshwater Molasse (=top Innviertel Group) and a thickness-contour-map of the Innviertel Group have been compiled (Fig. 4b–d).

Figure 4b shows the elevation of the smoothed base of the Innviertel Group. The general trend of this surface reflects the morphological evolution reasonably. The elevation increases gradually from west to east from –300 m to +300 m a.s.l. (above sea-level). The Upper Freshwater Molasse is only preserved in the eastern part of the study area. There the elevation of its base shows a similar trend to the base of the Innviertel Group and increases eastwards from +300 m to +600 m a.s.l. (Fig. 4c). The intersection of both horizon maps with the seismic line is also displayed in Fig. 5.

The thickness-contour-map of the Innviertel Group shows a rather uniform thickness of 550 to 600 m along the basin axis (W-E direction; Fig. 4d).

This suggests that (1) the effect of erosion during Karpatian time before deposition of the Upper Freshwater Molasse was minor and (2) that the Ottnangian Innviertel Group was tilted together with the Hall Formation.

Moisture content of Hausruck and Trimmelkam lignite

The average moisture content of Pannonian-age Hausruck lignite is 44.2 % (af) (standard deviation: 2.05 %; Pohl 1968). Considering the moisture depth trend for the Lower Rhine Embayment (Fig. 6), this value suggests burial of the Hausruck lignite beneath an overburden about 650 m thick. The present-day elevation of the Hausruck lignite seams varies between 580 and 650 m a.s.l. This suggests a Late Miocene paleo-land-surface at about 1250 m a.s.l., which is in contrast to the highest present-day elevation in the Hausruck

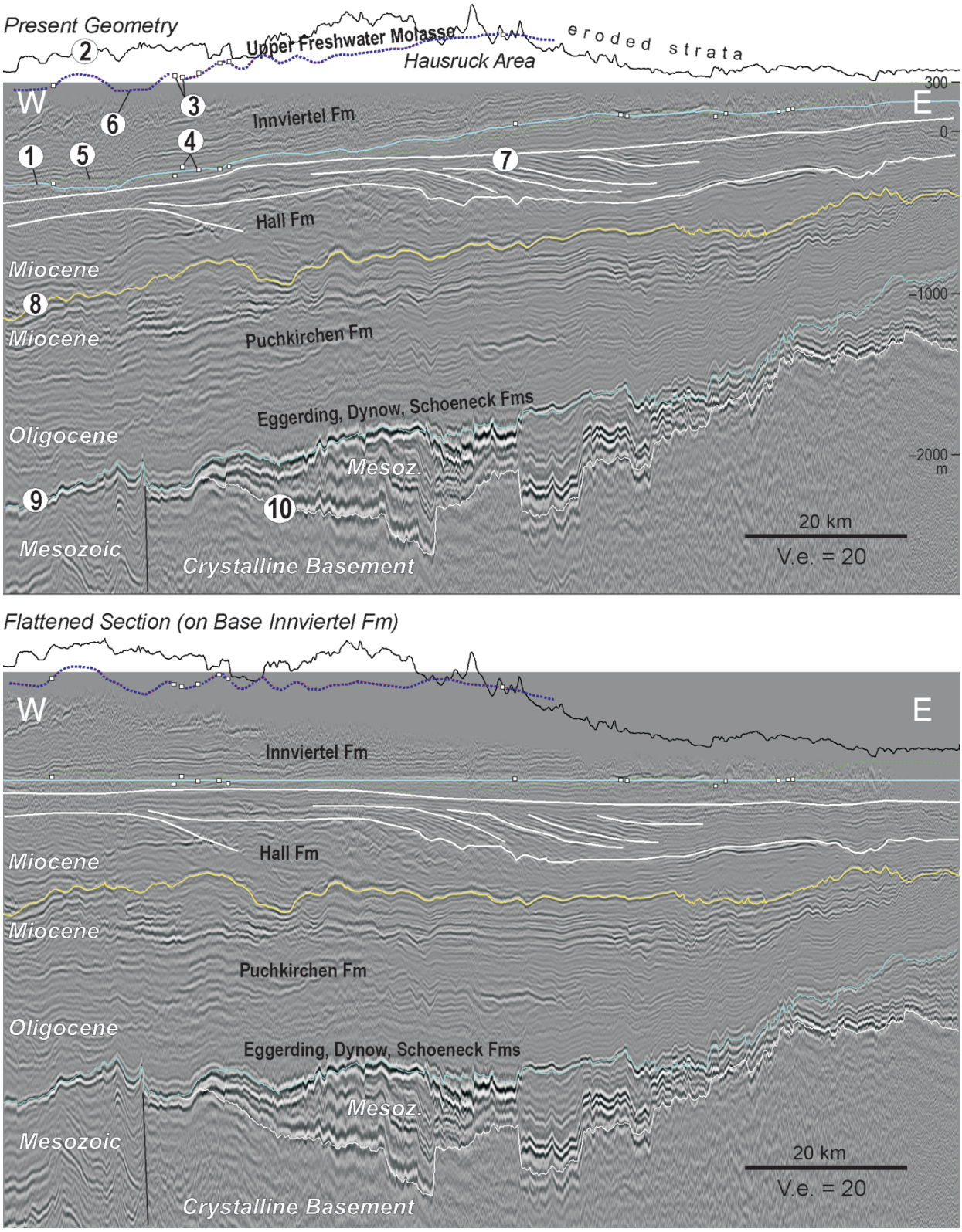

Fig. 5. Regional W-E 3D-reflection-seismic section in depth (vertical exaggeration 20 times, for position see Figure 1) showing the present day geometry (upper section) and the geometry "flattened" on the interpreted base of the Innviertel Group (point 1) in the lower section. The morphology (point 2) is created from SRTM 2004 data. Small squares represent projected well-tops of Base of Upper Freshwater Molasse and Base of Innviertel Group (points 3 and 4 respectively) as well as the interpolated surfaces (dotted lines, points 5 and 6, cf. Figure 4b,c). The prograding system in the Hall Formation is indicated (point 7). Additional regional horizons marked are Base of Hall unconformity (point 8), Top of Eocene (point 9) and Top of Crystalline Basement (point 10).

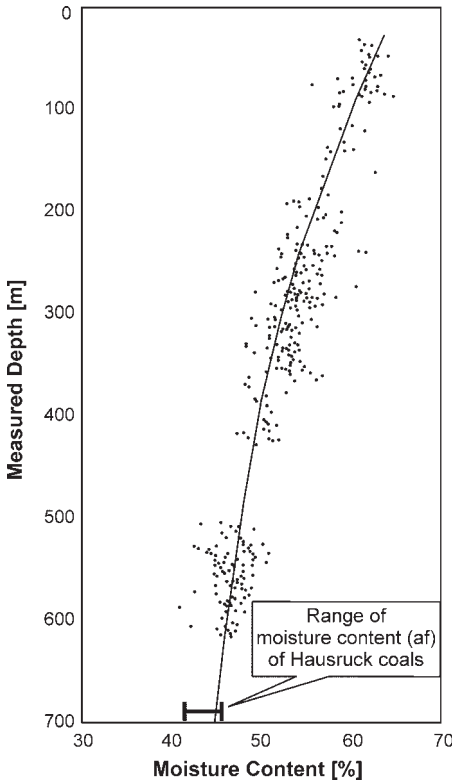

Fig. 6. Moisture depth trend of lignite from the Lower Rhine Embayment (after Kothen & Reichenbach 1981).

area of 801 m a.s.l. (Goebelberg). Uncertainties of the erosion estimate are related to the influence of coal facies on moisture depth trends and the role of erosion in the Lower Rhine Embayment. In any case, the moisture content in the Hausruck lignite implies extensive uplift and erosion.

Lignite in the Trimmelkam area is characterized by even lower moisture contents of (~35 % af; Weber & Weiss 1983). Unfortunately, Fig. 6 cannot be used to estimate the thickness of the original overburden. However, the lower moisture content well agrees with the lower elevation of the Trimmelkam lignite (300–350 m a.s.l.) and might be a result of burial beneath nearly 1000 m of overburden. Note, that the low moisture content of the Trimmelkam lignite has been previously explained by the pressure effect of the Pleistocene Salzach Glacier. However, the Salzach Glacier only reached a maximum thickness of 600 m in the Trimmelkam area (van Husen 1987).

Fission track data (U-Th/He; AFT, AHe)

The AFT and AHe data of sample Per-001 (1600 m; Upper Puchkirchen Formation) are rather consistent (Table 1). The apparent AFT age is older than the age of deposition (55 Ma vs. 22 Ma), but the mean track length shows significant shortening (12.8 μm). This is an indication of a young thermal overprint. The AHe ages also prove thermal reset;

Table 1: Apatite fission track and apatite (U-Th)/He (AFT and AHe, respectively) results from the Per-001 borehole (measured depth 1600 m; position in Figure 1).

		He		U238			Th232			Th/U	Sm			Ejection	*Uncorr.*	Ft-Corr.		Sample
Sample	aliq.	vol. [ncc]	s.e. [ncc]	mass [ng]	s.e. [%]	conc. [ppm]	mass [ng]	s.e. [%]	conc. [ppm]	ratio	mass [ng]	s.e. [%]	conc. [ppm]	correct. (Ft)	*He-age [Ma]*	*He-age* [Ma]	1s [Ma]	unweighted aver. & s.e.
Per1 1598.5–	#1	**0.023**	4.691	**0.040**	2.1	7.0	**0.048**	2.5	8.4	1.203	**0.104**	7.6	18	**0.720**	3.7	**5.1**	0.3	
–1601.5 K7 Ki2	#3	**0.042**	3.497	**0.042**	2.1	11.1	**0.173**	2.4	46.2	4.160	**0.693**	7.4	185	**0.598**	*4.0*	**6.6**	0.5	
	#5	**0.142**	2.274	**0.090**	1.9	8.1	**0.339**	2.4	30.4	3.767	**2.942**	7.7	264	**0.767**	*6.0*	**7.9**	0.4	
	#6	**0.005**	10.140	**0.011**	4.3	5.0	**0.012**	3.0	5.5	1.096	**0.089**	8.5	42	**0.588**	2.7	**4.6**	0.6	**6.1** 0.7

Amount of helium is given in nano-cubic-cm in standard temperature and pressure
Amount of radioactive elements are given in nanograms
Ft: alpha-ejection correction (according to Farley 2002)
Error on sample average age is 1 σ, as $(SD)/(n)^{1/2}$; where SD=standard deviation of the age replicates and *n* =number of age determinations.

	Cryst.	Spontaneous	Induced	Dosimeter	$P(\chi^2)$	Disp.	FT age*	Track length	Dpar
Sample		ρs (Ns)	ρi (Ni)	ρi (Ni)	[%]		[Ma ± 1s]	[μm, n]	[μm]
Per1 1598.5–									
–1601.5 K7 Ki2	20	7.09 (571)	13.0 (1044)	6.29 (4638)	64	0.02	**55.4**	**3.1** 12.8 ± 1.1 (53)	1.99 ± 0.25

Cryst: number of dated apatite crystals
Track densities (ρ) are as measured (x10^5 tr/cm^2); number of tracks counted (N) shown in brackets
$P(\chi^2)$: probability obtaining Chi-square value for n degree of freedom (where n = no. crystals-1)
Disp.: Dispersion, according to Galbraith & Laslett (1993)
*: Central ages

they are clearly younger than the age of deposition (single-grain ages are between 4.6 and 7.9 Ma).

For the proper interpretation of the detected rejuvenations in the thermochronometers several modelling runs of the thermal history were performed. For the modelling we have used the computer program HeFTy (Ketcham 2005). This forward modelling algorithm considers the apparent AFT age, track length distribution (Fig. 7), the angle of confined tracks relative to the crystallographic C-axis, kinetic parameters (Dpar), AHe ages and the geometry and actinide concentrations of the dated apatite crystals. For the modelling we only considered the age of sedimentation (22 Ma at 16 °C) and the current borehole temperature (ca. 55 °C) as invariable time-temperature points. The pre-depositional cooling age of the apatite grains was assumed to be between 100 and 60 Ma, because it is a dominant cooling age phase in the Eastern Alps, which is the major source area of the sediment.

The thermal modelling indicates a remarkable turn in the post-depositional thermal history. The rather rapid increase of the burial temperature was terminated around 10 Ma ago and since ca. 8 Ma the temperature decreases. Another less pronounced turn can also be observed at ca. 5 Ma. Since that time the temperature conditions are rather stable. However we should consider that this last turn is already in the less sensitive time-temperature range of the thermochronometers, thus this turn is much less constrained than the turn in the trend at ca. 10 Ma ago.

The enveloping of the acceptable tT paths (goodness of fit: GOF >0.05) is represented by a light grey field (Fig. 7) and the envelope of 'good fits' (GOF >0.5) by a black belt. These areas do not include those individual paths that offer numerically correct solutions, but tT paths, which are geologically meaningless. For example, paths showing extremely quick rate of post-depositional warming or indicating sharp turns (running in zigzags) were not considered.

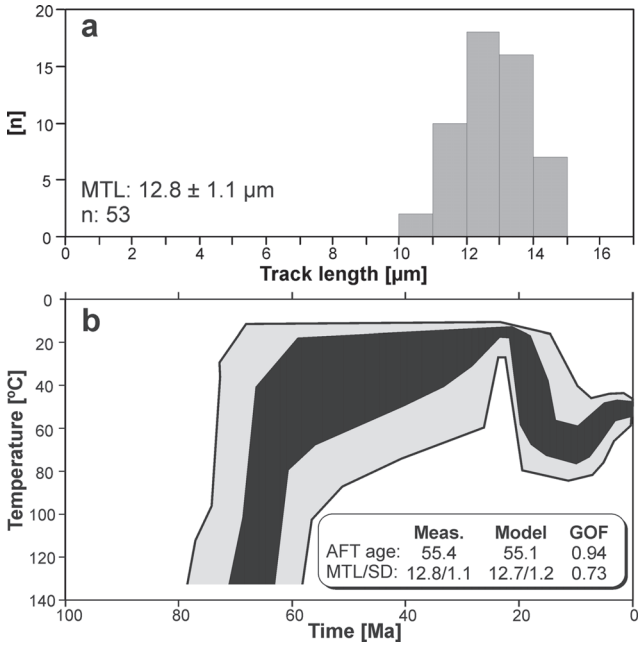

Fig. 7. a — Confined horizontal track lengths in the apatite crystals from the Per-001 borehole, measured depth 1600 m (position in Fig. 1). **b** — Time-temperature plot showing the results of the thermal modelling performed with HeFTy software (Ketcham 2005).

Discussion

The integration of the different data sets allows the separation of at least two tectonic events during Neogene times:

Karpatian/Badenian westward tilting

A regional Miocene westward tilting event affecting the Austrian part of the Molasse Basin is strongly indicated by the tilting of progradational patterns within the Hall Formation (Eggenburgian). The uniform thickness of Ottnangian sediments of the Innviertel Group along the basin axis suggests that the tilting occurred after Ottnangian time. The onlap relation of Lower Badenian to Pannonian rocks of the Upper Freshwater Molasse and the top of the Innviertel Group suggests that tilting occurred before the Badenian. Thus, the tilt of about 0.5 % can be attributed to the Karpatian. There is no regular change in the amount of Karpatian erosion along the E-W trending basin axis. This suggests that tilting postdates erosion.

Late Miocene regional uplift

Moisture contents of lignite in the Hausruck mining district suggest that the hypothetical Late Miocene paleo-land-surface is located at about 1250 m a.s.l. This implies major erosion after deposition of the Upper Freshwater Molasse in post-Early Pannonian times. Erosion removed 450 (Goebelberg area) to 800 m (valley areas between Trimmelkam and Hausruck) thick sediments.

Late Miocene to Pliocene cooling, as indicated by thermochronological data, supports regional exhumation after 10 million years before present. Although the amount of cooling is poorly constrained, its most likely value of about 20 °C (Fig. 7) fits well with an erosion in the order of 500 to 700 m (in consideration of typical geothermal gradients for this part of the basin of about 3.0 °C/100 m; Kamyar 2000). Moreover, the modelling results suggest that cooling reached a peak before 5 Ma.

Local uplift in the eastern Molasse Basin

Shale compaction data suggest that erosion in the eastern part of the study area removed sediments, which are up to 1000 m thicker than in the main part. Thus sediments in the order of 1500 to 1800 m thick were probably eroded. Although thermochronological data are missing, we assume that uplift was contemporaneous with regional uplift in the Late Miocene.

Comparison with Neogene uplift in the Swiss part of the Molasse Basin

For the Swiss part of the Alpine Foreland Basin eroded rocks at least 2 km thick related to a Late Miocene uplift

event have been proved (Kuhlemann & Kempf 2002). Schegg & Leu (1998) clarify the thicknesses of eroded Neogene sediments with values of 700 m in the northeast and 1500–3000 m near the Alpine front to the south. Numerous analyses on mineral cooling ages demonstrate that the basin underwent the erosion during Pliocene times. Concerning the cause of the uplift it is proposed that accelerated erosional unroofing of the Swiss Alps triggered isostatic rebound and erosion of the foreland basin after 5 Ma. Additionally a change in climate and/or drainage reorganization is suggested (Cederbom et al. 2004, 2011). Andeweg & Cloetingh (1998) propose that the Late Cenozoic uplift, which superimposes the former flexural process due to loading, might have been caused by breaking up or delamination of part of the subsided European crust.

Consequences for hydrocarbon systems in the Molasse Basin

Changes in basin geometry have an influence on both thermogenic and biogenic hydrocarbon systems. Tilting of the basin shifts oil–water contacts and controls migration paths. Basin uplift and erosion may cause termination of hydrocarbon generation if the system leaves the oil window (due to temperature decrease) along the way. Cooling favours biodegradation processes and biogenic gas generation. Decreasing pressure changes the gas–oil ratio. Upcoming basin and petroleum systems modelling based on structural forward modelled sections will provide information about these issues.

Possible mechanism for Neogene tectonic activity

A main extensional phase captured the region during Late Ottnangian or Karpatian to Early Badenian times. East of the Tauern window a number of intramontane pull-apart basins were formed along major stike-slip fault zones (e.g. Mur-Mur-Mürz-valley, Enns-valley). Due to these tectonic movements, stress regimes and sedimentation patterns significantly changed in the central and eastern part of the Eastern Alps (Frisch et al. 1998) and may also have affected the foreland basin even though in a minor way.

Peresson & Decker (1997) proposed that a Late Miocene (after 9 Ma and prior to 5.3 Ma) compressional event along the entire Alpine-Pannonian system terminated the former eastward lateral extrusion and reversed the stress regime.

The cause for prominent Neogene uplift in the Alpine region is still intensively discussed. It is probably related to isostatic rebound of the Alps after termination of thrusting. Cederbom et al. (2004) suggest that erosional unroofing of the Swiss part of the North Alpine Foreland Basin occurred due to isostatic rebound of the mountain belt in response to a wetter climate (driven by increased precipitation) post 5 Ma.

The strong local uplift in the eastern Molasse Basin parallels the southwestern margin of the Bohemian Spur. This spur exhibiting thickened crystalline crust extends some 100 km to the southeast below the Eastern Alps (see inset in Fig. 1 for location of the Bohemian Spur) (e.g. Tari 2005). Thus, isostatic uplift of the Bohemian Spur might have caused the observed differential uplift. Within this context, uplift data from the eastern margin of the Bohemian Spur would be interesting. According to our knowledge such data are not available.

Conclusion

The combination of geophysical, petrophysical and thermochronological techniques provides new insights into the timing and dimensions of uplift and erosion events in the Austrian part of the Northern Alpine Foreland Basin. The most important conclusions drawn from the present study include:

• An inclined toplap surface within the Hall Formation and the geometry of the Innviertel Group provide evidence for regional westward tilting of the study area. The gradient of the slope is about 5 m per kilometer (0.5 %). Tilting occurred during Karpatian time (~17 Ma before present) and postdates the Late Ottnangian filling of the marine basin. Tilting might be related to the contemporaneous onset of continental escape within the Eastern Alps. As a result of tilting, Badenian to Pannonian sediments of the Upper Freshwater Molasse onlap onto the inclined top Innviertel unconformity.

• Moisture contents of lignite in the Hausruck mining district and thermochronological (apatite fission track and (U-Th)/He) data from a sample in the western part of the study area indicate uplift and erosion after deposition of the Upper Freshwater Molasse. Erosion estimates are in the order of 500 to 900 m. Major erosion probably commenced at about 8 Ma and slowed down about 4 Ma before present. Although poorly constrained, this time interval excellently fits with the time constraints of Cederbom et al. (2004) and Genser et al. (2007) although the thicknesses of eroded rocks reach greater dimensions in the Swiss part of the basin.

• Shale compaction data have been derived from sonic logs of the Eggerding Formation (Lower Oligocene). Most data follow a regular depth trend. Deviations from this trend indicate that uplift along a narrow zone in the easternmost part of the study area was significantly higher (up to 1000 m) than in the rest of the study area. Considering the regional uplift of 500 to 900 m, it is concluded that sediments, up to 1500 or even 1900 m thick, have been eroded along the narrow eastern zone. It is reasonable to assume that eastern uplift was contemporaneous with regional uplift (i.e. Late Miocene). Uplift in the east is probably related to differential isostatic rebound of the crystalline rocks along the Bohemian Spur compared to clastic basin fill or to a compressional event (Peresson & Decker 1997).

• We can expect that both Karpatian tilting and Late Miocene erosion have major influence on the petroleum systems. For example, tilting probably influenced oil–water contacts in E-W-elongated hydrocarbon deposits. Moreover uplift and erosion probably stopped hydrocarbon generation and influenced gas to oil ratios in existing accumulations.

Acknowledgments: We thank RAG AG for their permission to publish the data. Special thanks go to RAG geological personnel for constructive discussion inputs. For helpful comments concerning the moisture content of coal we are notably thankful to Bernhard Salcher (ETH Zürich). The

manuscript benefited from the useful comments of the reviewers, Gabor Tari (OMV) and Nestor Oszczypko (Jagiellonian University Krakow).

References

Andeweg B. & Cloetingh S.A.P.L. 1998: Flexure and 'unflexure' of the North Alpine German-Austrian Molasse Basin: constraints from forward tectonic modelling. In: Mascle A., Puigdefàbregas C., Luterbacher H.P. & Fernandez M. (Eds.): Cenozoic foreland basins of Western Europe. *Geol. Soc., Spec. Publ.* 134, 403–422.

Bachmann G.H., Mueller M. & Weggen K. 1987: Evolution of the Molasse Basin (Germany, Switzerland). *Tectonophysics* 137, 77–92.

Cederbom C.E., Sinclair H.D., Schlunegger F. & Rahn M.K. 2004: Climate induced rebound and exhumation of the European Alps. *Geology* 32, 709–712.

Cederbom C.E., Van der Beek P., Schlunegger F., Sinclair H.D. & Oncken O. 2011: Rapid extension erosion of the North Alpine foreland basin at 5–4 Ma. *Basin Research* 23, 528–550.

Czurda K. 1978: Sedimentologische Analyse und Ablagerungsmodell der miozänen Kohlemulden der oberösterreichischen Molasse. *Jb. Geol. B.-A.* 121, 123–154.

De Ruig M.J. & Hubbard S.M. 2006: Seismic facies and reservoir characteristics of a deep marine channel belt in the Molasse foreland basin. *AAPG Bull.* 90, 735–752.

Donelick R.A., Ketcham R.A. & Carlson W.D. 1999: Variability of apatite fission-track annealing kinetics. II. Crystallographic orientation effects. *Amer. Mineralogist* 84, 9, 1224–1234.

Dumitru T.A. 1993: A new computer-automated microscope stage system for fission-track analysis. *Nucl. Tracks Radiat. Meas* 21, 575–580.

Farley K.A. 2002: (U-Th)/He dating: techniques, calibrations, and applications. *Rev. Mineral. Geochem.* 47, 819–844.

Faupl P. & Roetzel R. 1987: Gezeitenbeeinflusste Ablagerungen der Innviertler Gruppe (Ottnangian) in der österreichischen Molassezone. *Jb. Geol. B.-A.* 130, 415–447.

Frisch W., Kuhlemann J., Dunkl I. & Brügel A. 1998: Palinspastic reconstruction and topographic evolution of the Eastern Alps during late Tertiary tectonic extrusion. *Tectonophysics* 297, 1–15.

Genser J., Cloetingh S.A.P.L. & Neubauer F. 2007: Late orogenic rebound and oblique Alpine convergence: New constraints from subsidence analysis of the Austrian Molasse basin. *Glob. Planet. Change* 58, 214–223.

Gleadow A.J.W. & Duddy I.R. 1981: A natural long-term track annealing experiment for apatite. *Nuclear Tracks* 5, 169–174.

Groiss R. 1989: Geologie und Kohlebergbau im Hausruck (Oberösterreichische Molasse). *Arch. f. Lagerst. Forsch. Geol. B.-A.*, Wien 11, 167–178.

Grunert P., Soliman A., Harzhauser M., Müllegger S., Piller W.E., Roetzel R. & Rögl F. 2010: Upwelling conditions in the Early Miocene Central Paratethys sea. *Geol. Carpathica* 61,129–145.

Grunert P., Soliman A., Ćorić S., Roetzel R., Harzhauser M. & Piller W.E. 2012: Facies development along the tide-influenced shelf of the Burdigalian Seaway: An example from the Ottnangian-stratotype (Early Miocene, middle Burdigalian). *Mar. Micropaleont.* 84–85, 14–36.

Gusterhuber J., Sachsenhofer R.F. & Linzer H.-G. 2011: A 2D basin and petroleum systems modelling study in an overthrust setting — The Alpine Molasse Basin, Austria. *73rd EAGE Conference & Exhibition incorporating SPE EUROPEC 2011 Vienna*, 1–257.

Hinsch R. 2008: New insights into the Oligocene to Miocene geological evolution of the Molasse Basin of Austria. *Oil & Gas European Mag.* 34, 3, 138–143.

Hubbard S.M., De Ruig M.J. & Graham S.A. 2009: Confined channel-levee complex development in an elongate depo-center: Deep-water Tertiary strata of the Austrian Molasse basin. *Mar. Petrol. Geol.* 26, 85–112.

Hurford A.J. 1998: Zeta: the ultimate solution to fission-track analysis calibration or just an interim measure? In: Van den Haute P. & De Corte F. (Eds.): Advances in fission-track geochronology. *Kluwer Academic Publishers*, 19–32.

Hurford A.J. & Green P.F. 1983: The zeta age calibration of fission-track dating. *Chem. Geol., Isot. Geosci.* 41, 285–312.

Issler D.R. 1992: A new approach to shale compaction and stratigraphic restoration, Beaufort-Mackenzie Basin and Mackenzie Corridor, Northern Canada. *AAPG Bull.* 76, 1170–1189.

Kamyar H.R. 2000: Verteilung der Untergrundtemperarturen an den Beispielen der Bohrlochtemperatur (BHT) — Messungen in den RAG Konzessionen, Oberösterreichs und Salzburgs, (Molasse- und Flyschzone). *PhD Thesis, Univ. Vienna*, 1–145.

Ketcham R.A. 2005: Forward and inverse modeling of low-temperature thermochronometry data. *Rev. Mineral. Geochem.* 58, 275–314.

Kothen H. & Reichenbach K. 1981: Teufenabhängigkeit und gegenseitige Beziehungen von Qualitätsparametern der Braunkohle der Niederrheinischen Bucht. *Fortschr. Geol. Rheinland. Westfalen* 29, 353–380.

Krenmayer H.G. 1999: The Austrian sector of the North Alpine Molasse: A classic foreland basin. *FOREGS* (*Forum of Euopean Geological Surveys*) Dachstein-Hallstatt-Salzkammergut Region, Vienna, 22–26.

Kuhlemann J. & Kempf O. 2002: Post-Eocene evolution of the North Alpine Foreland Basin and its response to Alpine tectonics. *Sed. Geol.* 152, 45–78.

Linzer H.-G. 2002: Structural and stratigraphic traps in channel systems and intraslope Basins of the deep-water molasse foreland Basin of the Alps. *AAPG Search and Discovery Article #90007 AAPG Annual Meeting Houston*, Texas, 1–2.

Magara K. 1976: Thickness of removed sedimentary rocks, paleopore pressure, and paleotemperature, Southwestern Part of Western Canada Basin. *AAPG Bull.* 60, 554–565.

Magara K. 1980: Comparison of porosity-depth relationships of shale and sandstone. *J. Petrol. Geol.* 3, 175–185.

Malzer O., Rögl F., Seifert P., Wagner L., Wessely G. & Brix F. 1993: Die Molassezone und deren Untergrund. In: Brix F. & Schultz O. (Eds.): Erdöl und Erdgas in Österreich. *Naturhist. Mus. Wien und F. Berger*, 281–358.

Nachtmann W. & Wagner L. 1987: Mesozoic and Early Tertiary evolution of the Alpine foreland in Upper Austria and Salzburg, Austria. *Tectonophysics* 137, 61–76.

Peresson H. & Decker K. 1997: Far-field effects of Late Miocene subduction in the Eastern Carpathians: E-W compression and inversion of structures in the Alpine-Carpathian-Pannonian region. *Tectonics* 16, 38–56.

Pohl W. 1968: Zur Geologie und Paläogeographie der Kohlemulden des Hausruck (O.Ö.). *PhD Thesis, Univ. Vienna* 17, 70.

Rögl F. 1998: Palaeogeographic Considerations for Mediterranean and Paratethys Seaways (Oligocene to Miocene). *Ann. Naturhist. Mus. Wien* 99A, 279–310.

Rögl F. 1999: Mediterranean and Paratethys. Facts and hypothesis of an Oligocene to Miocene Paleogeography (short overview). *Geol. Carpathica* 50, 4, 339–349.

Rupp C., Hofmann T., Jochum B., Pfleiderer S., Schedl A., Schindlbauer G., Schubert G., Slapansky P., Tilch N., Husen D. van, Wagner L. & Wimmer-Frey I. 2008: Geologische Karteder Republik Österreich 1:50,000, Blatt 47 Ried im Innkreis. Erläuterungen zu Blatt 47 Ried im Innkreis. *Geol. Surv. Austria*, Vienna.

Sachsenhofer R.F., Leitner B., Linzer H.-G., Bechtel A., Ćorić S., Gratzer R., Reischenbacher D. & Soliman A. 2010: Deposition,

erosion and hydrocarbon source potential of the Oligocene Eggerding Formation (Molasse Basin Austria). *Austrian J. Earth Sci.* 103, 76–99.

Schegg R. & Leu W. 1998: Analysis of erosion events and paleogeothermal gradients in the North Alpine Foreland Basin of Switzerland. In: Düppenbecker S.J. & Iliffe J.E. (Eds.): Basin modelling: Practice and progress. *Geol. Soc. London* 141, 137–155.

Schulz H.-M., Sachsenhofer R.F., Bechtel A., Polesny H. & Wagner L. 2002: Origin of hydrocarbon source rocks in the Austrian Molasse Basin (Eocene-Oligocene transition). *Mar. Petrol. Geol.* 19, 6, 683–709.

Schulz H.-M., Bechtel A. & Sachsenhofer R.F. 2005: The birth of the Paratethys during the Early Oligocene: From Tethys to an ancient Black Sea analogue? *Glob. Planet. Change* 49, 163–176.

SRTM 2004: Void-filled seamless SRTM data V1 (2004) International centre for tropical agriculture (CIAT). Available from the CGIAR-CSI SRTM 90 m Database: http://srtm.csi.cgiar.org and http://www.ambiotek.com/topoview

Tari G. 2005: The divergent continental margins of the Jurassic Proto-Pannonian Basin: Implications for the petroleum systems of the Vienna Basin and the Moesian Platform. *25th Annual Bob F. Perkins Research Conference: Petroleum Systems of Divergent Continental Margins*, Houston.

Van Husen D. 1987: Die Ostalpen inden Eiszeiten. *Populärwissenschaftliche Veröffentlichungen der Geologischen Bundesanstalt*, (Map 1:500,000), Vienna.

Wagner L.R. 1996: Stratigraphy and hydrocarbons in the Upper Austrian Molasse Foredeep (active margin). In: Wessely G. & Liebl W. (Eds.): Oil and gas in Alpidic Thrustbelts and Basins of Central and Eastern Europe. *EAGE Spec. Publ.* 5, 217–235.

Wagner L.R. 1998: Tectono-stratigraphy and hydrocarbons in the Molasse foredeep of Salzburg, Upper and Lower Austria. In: Mascle A., Puigdefàbregas C., Luterbacher H.P. & Fernandez M. (Eds.): Cenozoic Foreland Basins of Western Europe. *Geol. Soc., Spec. Publ.* 134, 339–369.

Weber L. & Weiss A. 1983: Bergbaugeschichte und Geologie der österreichischen Braunkohlevorkommen. *Arch. f. Lagerst. Forsch. Geol. B.-A.*, Wien 4, 317.

Wells P.E. 1990: Porosities and seismic velocities of mudstones from Wairarapa and oil wells of North Island, New Zealand, and their use in determining burial history. *New Zealand J. Geol. Geophys.* 33, 29–39.